

Study of a hydrogen-bombardment process for molecular cross-linking within thin films

Y. Liu,¹ D. Q. Yang,² H.-Y. Nie,² W. M. Lau,² and J. Yang^{1,a)}

¹*Department of Mechanical and Materials Engineering, University of Western Ontario, London, Ontario, Canada*

²*Surface Science Western, University of Western Ontario, London, Ontario, Canada*

(Received 16 November 2010; accepted 24 January 2011; published online 16 February 2011)

A low-energy hydrogen bombardment method, without using any chemical additives, has been designed for fine tuning both physical and chemical properties of molecular thin films through selectively cleaving C–H bonds and keeping other bonds intact. In the hydrogen bombardment process, carbon radicals are generated during collisions between C–H bonds and hydrogen molecules carrying ~ 10 eV kinetic energy. These carbon radicals induce cross-linking of neighboring molecular chains. In this work, we focus on the effect of hydrogen bombardment on dotriacontane ($C_{32}H_{66}$) thin films as growing on native SiO_2 surfaces. After the hydrogen bombardment, XPS results indirectly explain that cross-linking has occurred among $C_{32}H_{66}$ molecules, where the major chemical elements have been preserved even though the bombarded thin film is washed by organic solution such as hexane. AFM results show the height of the perpendicular phase in the thin film decreases due to the bombardment. Intriguingly, Young's modulus of the bombarded thin films can be increased up to ~ 6.5 GPa, about five times of elasticity of the virgin films. The surface roughness of the thin films can be kept as smooth as the virgin film surface after thorough bombardment. Therefore, the hydrogen bombardment method shows a great potential in the modification of morphological, mechanical, and tribological properties of organic thin films for a broad range of applications, especially in an aggressive environment. © 2011 American Institute of Physics. [doi:10.1063/1.3554430]

I. INTRODUCTION

There has been a remarkable growth of applications of organic thin films over the past years, such as wetting control,¹ biotechnology,² organic electronics,^{3,4} optics and photonics,^{5,6} data storage,^{7,8} and chemical sensors.^{9,10} These applications need novel surface techniques to modify physical and/or chemical properties of thin films to meet various requirements. Traditional approaches for molecular cross-linking on a surface are wet chemical processes that rely on reactions of radicals and/or ions with organic molecules.^{11–15} In these processes, specific chemical additives are used to introduce reactive sites for cross-linking,¹² and consequently chemical disposal in general needs to be properly handled in the post processes.

To lessen chemical usage and disposal, one promising technique for surface modification has been invented using mass-separated ion beam to modify solid surfaces.¹⁶ In this study, we applied a newly developed process, a low-energy hydrogen bombardment method, to modify the physical properties of organic thin films. This method precisely controls charge-neutral hydrogen projectiles that carry ~ 10 eV kinetic energy to bombard thin films.

The principle of hydrogen bombardment is straightforward. According to the first-approximation of hard-sphere binary collision, when a projectile collides head-on with a target its energy can be most effectively transferred. The energy transfer fraction can be determined by $4M_t M_p / (M_t + M_p)^2$

(Refs. 17 and 18) as listed in Table I. Theoretically, the maximum energy transferred from a 10 eV hydrogen projectile to a hydrogen atom of a molecular chain is 10 eV. From the atomic point of view, the effective energy left after collision, between the hydrogen projectile and the H atom, can break a C–H bond whose bond energy is 4.3 eV as listed in Table II. However, if the 10 eV hydrogen projectile collides with a carbon atom of the molecular chain, the maximum energy transferred is only 2.8 eV, which is not enough to break a C–C bond with energy of 3.6 eV. The schematic illustration of the hydrogen bombardment process is depicted in Fig. 1.

The hydrogen bombardment method enables modification of physical properties of films without using any chemical additives. Because of the use of the charge-neutral hydrogen projectiles, this method largely alleviates the surface charging effect that is commonly found in conventional ion/plasma-based bombardments.^{19–22} In addition, this technique owns the potential to avoid dielectric damage on coatings especially in the applications of semiconductor industry.^{23,24}

Dotriacontane $C_{32}H_{66}$ is chosen as an example molecule system for studying this bombardment method. First, *n*-alkane molecules $CH_3(CH_2)_nCH_3$ have been recognized as main ingredients of organic and biological molecules,^{25,26} which have led to a great amount of theoretical and experimental researches in polymer science and engineering.^{27–29} They are also of industrial importance as lubricant additives in applications of adhesion, lubrication, and coatings.³⁰ Furthermore, since *n*-alkane molecules have linear molecular structure and

^{a)}Electronic mail: jyang@eng.uwo.ca.

TABLE I. Maximum energy transferred from projectiles to target atoms.

Atom–atom interaction	10 eV H → H	10 eV H → C	5 eV H → H	5 eV H → C	15 eV H → H	15 eV H → C
Transferred energy (eV)	10	2.8	5	1.4	15	4.3

have only saturated C–C, they are good sample molecules for characterizing our hydrogen bombardment process.

In addition, we have learned in literature that dotriacontane molecules as growing on SiO₂ can either perpendicularly stand up or lay down in parallel.³¹ They represent two phases of self-assembled monolayers (SAMs) with different molecular orientations: 0° and 90°. It has been known that alkanethiol monolayers, as growing on gold substrates, tilt with a certain angle in the range of 0°–90° depending on the chain lengths.³² Therefore, the two-phase nature of dotriacontane itself is attractive enough as a good candidate for research of SAMs as well, especially the mechanical properties.

Two characterization tools are used: x-ray photoelectron spectroscopy (XPS) and atomic force microscopy (AFM). XPS was first used to determine chemical content, i.e., carbon in this study. AFM was used as the major nanoscopic tool to interpret the physical effects of the low-energy hydrogen bombardment on the C₃₂H₆₆ thin films, i.e., morphological and mechanical properties at the nanoscale. Both contact and tapping AFM modes are generally applied to study thin layers from different aspects.^{33–36} In this paper torsional harmonic^{37,38} and force modulation³⁹ AFM modes were employed to characterize the mechanical strength of the dotriacontane thin films, before and after the hydrogen bombardment.

II. EXPERIMENTAL DESIGN AND METHOD

A 0.3 wt. % dotriacontane, CH₃(CH₂)₃₀CH₃, solution in hexane was spin coated on to a silicon (100) wafer covered by a native oxide layer. When the coating process was performed on a spin coater at a rotational speed 5000 rpm for 1 min, this concentration of dotriacontane solution can form “fractal-like island” monolayer as shown in Fig. 3. We had carried out topography and phase images at different sites on the samples and confirmed that under this condition there was only one perpendicular monolayer growing above parallel layers. This can also be concluded based on Figs. 6–8. Seven samples with different exposure times to hydrogen bombardment were prepared for experiment. Total two runs of experiments were carried for statistical analysis.

The low-energy hydrogen bombardment was performed with a home-built and low-cost mass-separated low energy ion beam system,^{16,18,40,41} which delivers a hydrogen beam to the target substrate in a high vacuum chamber. Hydrogen gas with the purity of 99.8% was used in the bombardments.

TABLE II. Bond energy for typical chemical bonds.

Chemical bond	C–H	C–C	C=C (π bond)
Bond energy (eV)	4.3	3.6	2.7

The final beam energy was controlled at ~10 eV and the full width at half maximum of the energy distribution of hydrogen molecules was less than 0.6 eV. The fluence was varied from 1×10^{16} to 1×10^{18} cm⁻² with the exposure times varying from 5 to 700 s, and other parameters of bombardment were kept same.

The morphology and mechanical properties of the monolayers were investigated in a commercially Dimension V with Nanoscope V controller from Veeco Inc., which was equipped with a quadrant photodetector for detecting the cantilever deflection.^{42,43} All AFM experiments were performed in an ambient environment. Rectangular silicon cantilevers from Nanoscience Instruments with nominal spring constant 0.03 and 3.0 N/m were used in contact mode for height measurements and tapping mode for roughness measurements, respectively. A diamond-coated cantilever with calibrated tip radius of 52 nm and spring constant of 0.23 N/m from Nanoscience Instruments was used in force modulation. The cantilever used in torsional harmonic has a T-shaped tip and the tip radius is 8 nm as calibrated by the blunt method in SPIP software (Image Metrology); and its spring constant of 2.76 N/m was calibrated by thermal fluctuation method.⁴⁴ We calibrated the Young’s modulus on polystyrene–low-density polyethylene (PS–LDPE) calibration sample (Veeco, Inc.) before, during, and after experiments. There was no significant change in the Young’s modulus for PS (~2 GPa) and LDPE (~0.1 GPa). It has proved that our AFM experimental results are reliable and consistent.

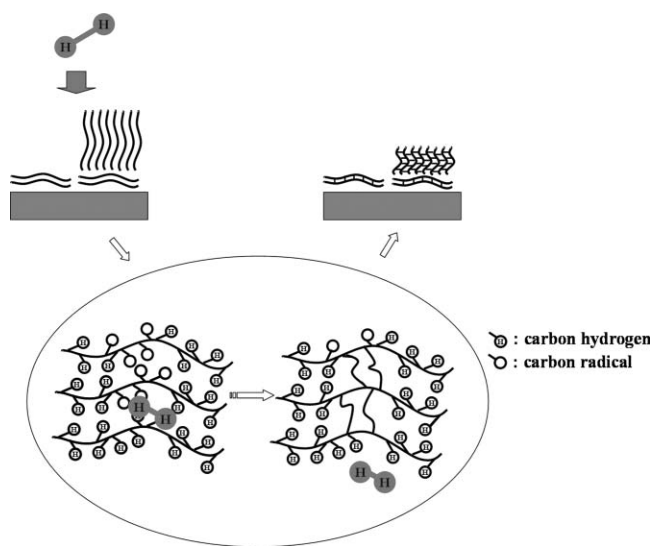


FIG. 1. Schematic illustration of the mechanism of hydrogen bombardment process for molecular cross-linking: generation of carbon radicals due to the low-energy hydrogen bombardment, formation of cross-link among molecular chains, and change of the height of the thin film due to the molecular cross-link.

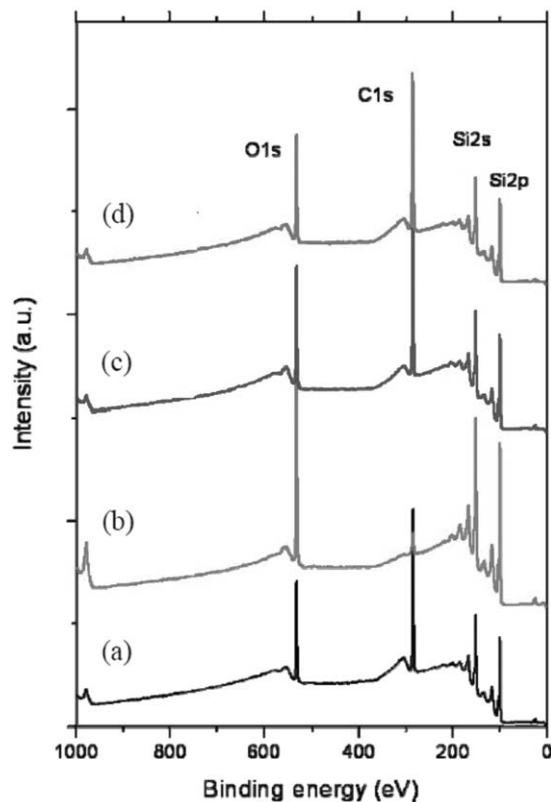


FIG. 2. XPS survey spectra of (a) virgin $C_{32}H_{66}$ monolayer; (b) the sample measured after immersion in hexane for 5 min; (c) $C_{32}H_{66}$ monolayer after 600 s bombardment; (d) the bombarded sample immersion in hexane for 5 min.

III. RESULTS AND DISCUSSIONS

A. X-ray photoelectron spectroscopy results

XPS spectra of thin films as prepared are displayed in Fig. 2, which were used for determining whether the chemical component retained after bombardment. The spectrum of virgin thin films [Fig. 2(a)] shows virtual C 1s signal from the $C_{32}H_{66}$ and Si 2s, Si 2p, and O 1s signals detected from the substrate. Without hydrogen bombardment, the thin films are soluble in hexane after immersion for 5 min, which is indicated by the significant reduction of the C 1s signal in XPS spectrum as shown in Fig. 2(b). However, for the thin films bombarded by a 10 eV hydrogen beam up to 600 s, no visible change in C 1s signal can be found comparing XPS spectrums before and after immersion in hexane as shown in Figs. 2(c). Therefore, it is reasonable to point out the occurrence of the cross-linking on the monolayers after being bombarded for 600 s. Such cross-linking is the cause that significantly enhances the insolubility of alkane thin film in hexane. This indicates potential applications of this technique for making organic thin films as coatings in severe environment. In addition, the XPS result (C 1s signals) shows that 10 eV hydrogen projectiles for bombardment cannot break C–C bonds and cause no main chain scission on the thin layers as mentioned before. So only breaking of C–H bonds is involved in the present process. We will present

AFM results to further illustrate physical effects of the hydrogen bombardment on morphological and mechanical properties of the treated thin films.

B. Effect of bombardment on thin film height and molecular density

At the microscopic viewpoint of surface science, the growth mechanism of *n*-alkane layers on SiO_2 surface has attracted increasing interest.^{27–29,45–47} Both of theoretical simulation⁴⁷ and experimental measurements^{48,49} confirmed such a structural model: one or two layers of $C_{32}H_{66}$ are immediately adsorbed on the SiO_2 surface with the long axis of the molecule parallel to the interface; and then additional layers of molecules are standing upright with the molecules' long axis oriented perpendicularly and all-trans length. As we mentioned before, these two phases, representing two cases of monolayer formation, need thorough analysis.

Due to different interactions of parallel and perpendicular layers exerting on the AFM tip, the amplitude-modulation tapping AFM mode measured “false step” heights of the all-trans and perpendicular monolayers formed on the SiO_2 substrate. The previous study using contact AFM measured the height of the all-trans conformation of the *n*-alkane molecular monolayer.⁴⁸ Here we confirmed the result by also utilizing the contact AFM mode for measuring the height of virgin $C_{32}H_{66}$ perpendicular monolayer before and after bombardment.

Through appropriate sample preparation, i.e., 0.3 wt. % dotriacontane and 5000 rpm spin-coating speed in ambient, perpendicular monolayer resembling fractal-like island was formed⁴⁶ as shown in Fig. 3. The height of perpendicular layer after bombardment was measured as a function of exposure or bombarding time. (Note: other operating parameters of bombardment were kept the same in this study so that the different exposure times corresponded to different hydrogen fluences.) The results of height measurement are shown in Fig. 4. The height of the virgin $C_{32}H_{66}$ monolayer was estimated to be 4.56 ± 0.19 nm, consistent with that of an all-trans conformation of the molecular monolayer ~ 44 Å as calibrated by high-resolution ellipsometry in literature.^{45,50} Through the hydrogen bombardment, the monolayer height decreases with the increase of exposure time as shown in Fig. 4. At and after 600 s exposure time, the molecular layer height becomes 2.58 ± 0.08 nm, only about 57% of the height of the virgin layer. However, our XPS result on the same sample shows that the estimated carbon concentration does not change with the exposure time. This comparison between AFM and XPS results suggest that the bombarded thin film becomes cross-linked and forms denser molecular networks as a result of cross-linked C–C bonds between molecular chains. It was further noticed that thorough bombardment (the exposure time larger than ~ 600 s) brought less variation in the height over the entire perpendicular layer. Nevertheless, for exposure time less than 600 s, e.g., between 50 s and 400 s, cross-linking was not fully saturated. As a result, the height of the entire thin film was nonuniform.

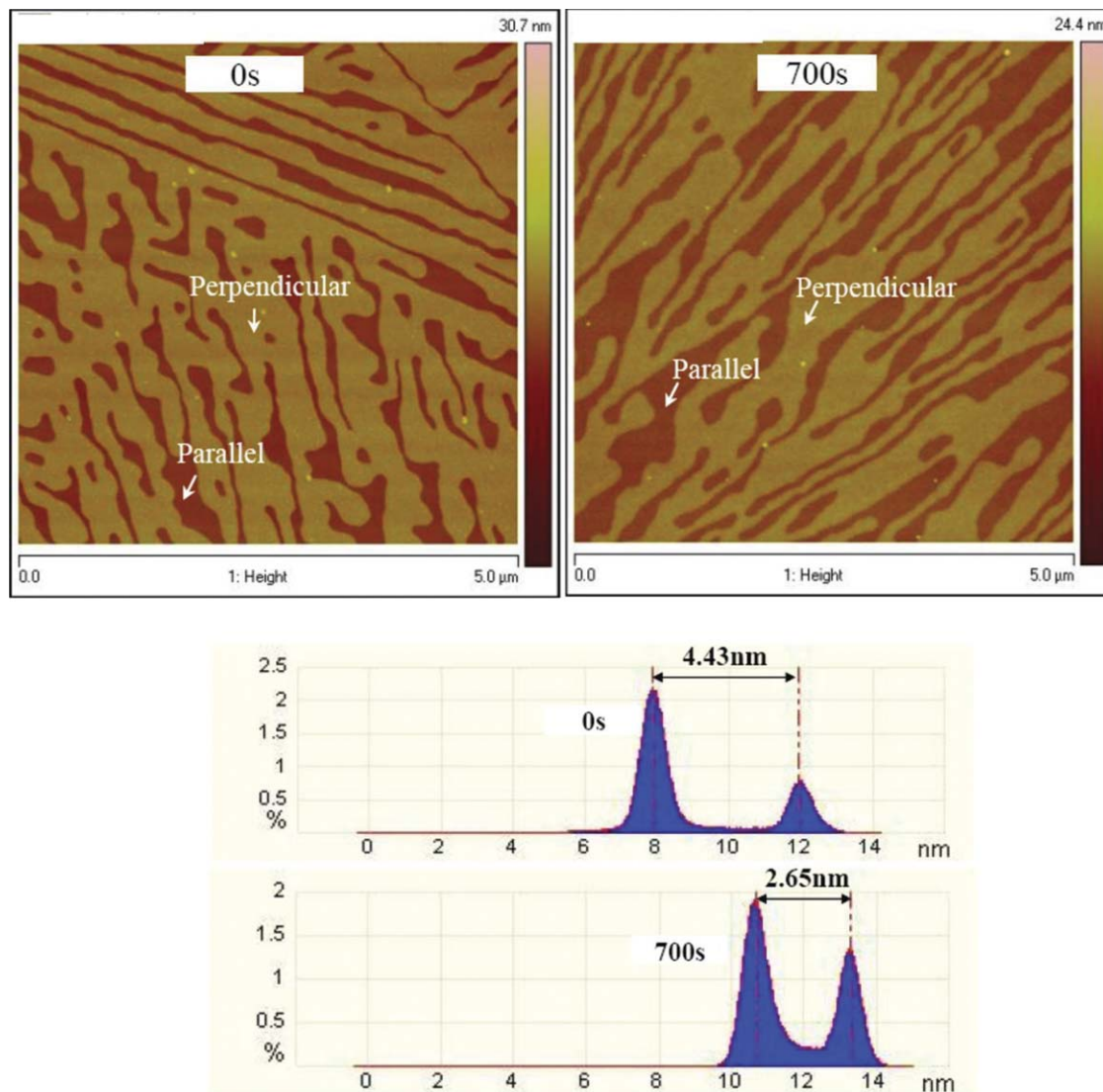


FIG. 3. Topographic images (top) and height (bottom) of $C_{32}H_{66}$ perpendicular monolayer without bombardment (0 s) and after 700 s bombardment.

C. Roughness measurements and critical exposure time

As shown in Fig. 4, 400 s might be the critical exposure time that corresponds to the necessary hydrogen fluence required for thorough bombardment on the $C_{32}H_{66}$ thin film. In this bombardment process, a bundle of hydrogen molecules are projected on the target. It is difficult to control the distribution of projectiles evenly on the sample surface and thus the collisions between hydrogen and C–H bonds are random. However, the effect of collisions could be quantitatively determined based on the roughness measurements through two runs of experiments in our study. The referred roughness is defined as⁵¹

$$R_a = \frac{1}{NM} \sum_{j=1}^M \sum_{i=1}^N |z_{ij} - z_{\text{average}}|. \quad (1)$$

The roughness R_a measurements were carried on the perpendicularly oriented monolayers with a constant scan area of $200 \text{ nm} \times 200 \text{ nm}$ for all of samples.⁵¹ Tapping mode

was adopted as the characteristic means because it gently tunes the tapping force exerted on the monolayer⁵² and owns statistical advantages to provide more reliable results.⁵³ As shown in Fig. 5, virgin $C_{32}H_{66}$ perpendicular monolayer has a very smooth surface of $R_a = 0.14 \pm 0.02 \text{ nm}$, which is very close to the roughness of the supporting silicon substrate, $\sim 0.1 \text{ nm}$ (Ref. 54). We noticed that the roughness on the bombarded surface increases with the increasing exposure times; and at $\sim 200 \text{ s}$, the roughness increased to a peak value at $R_a = 0.70 \pm 0.04 \text{ nm}$. After further increase of the exposure time beyond 200 s, the roughness started to decrease and eventually the surface becomes very smooth again with a stable $R_a \sim 0.15 \pm 0.01 \text{ nm}$ after the exposure time of $>400 \text{ s}$.

The results shown above suggest that, first, the thoroughly bombarded alkane thin film can have the same smoothness as the virgin film. Second, the exposure time $\sim 400 \text{ s}$ specifies the sufficient ion fluence required for achieving thorough bombardment of the $C_{32}H_{66}$ thin film. Finally, at 200 s exposure time, the roughness reaches the maximum

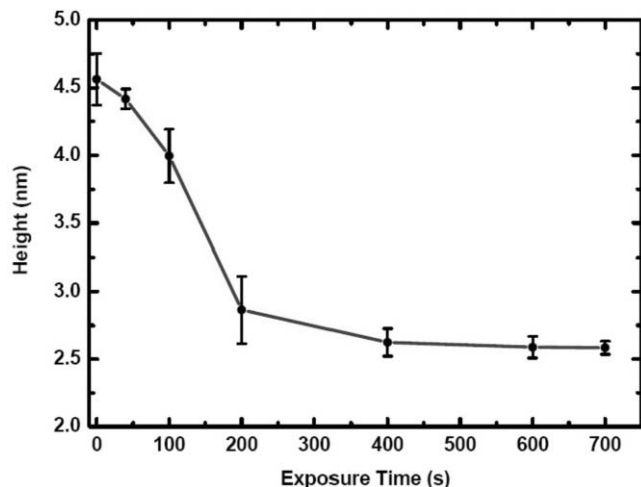


FIG. 4. AFM measurements show that the height of $C_{32}H_{66}$ perpendicular monolayer decreases as the exposure time increases.

value of ~ 0.70 nm, nearly five times larger than the roughness of the virgin surface. This corresponds to a case of partially bombarded surface (also shown in Fig. 4) for which the degree of cross-linking varies most significantly over the entire surface. This phenomenon can be further explained in such a way: in our experiments, $C_{32}H_{66}$ molecules initially stood perpendicularly on the substrate with an all-trans length; for a partial bombardment at the exposure time ~ 200 s, some molecules were cross-linked with each other and then bent down but other intact molecules were still standing perpendicularly with its full length. As a result, the partial bombardment produced a rugged surface and the roughness was high. Therefore, the roughness of the bombarded surface can be a useful parameter that indicates the degree of the molecular cross-linking due to the bombardment. The result of roughness measurement for the exposure time ~ 200 s is also consistent with the result of height measurement as shown in Fig. 4, where the standard deviation of the measured height is largest corresponding to the maximum value of roughness herein.

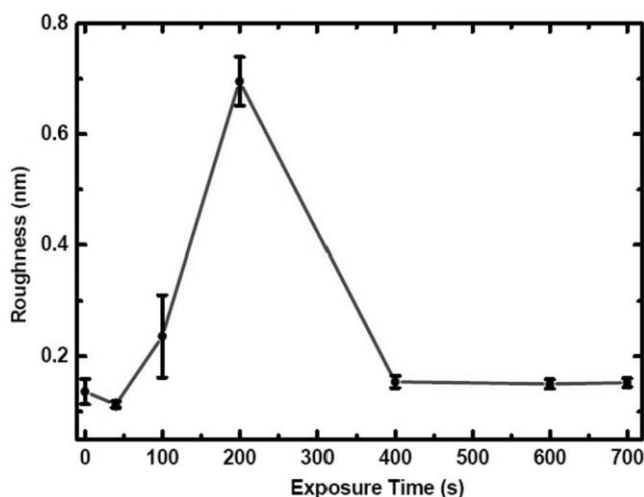


FIG. 5. Roughness variance of $C_{32}H_{66}$ perpendicular monolayer with respect to the exposure time (measured by AFM). The error bars represent the standard deviations of roughness of surface of seven bombarded samples.

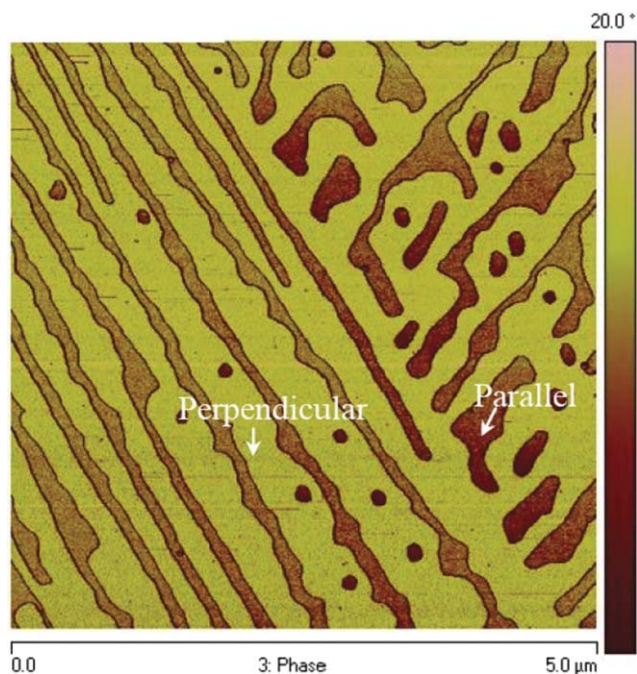


FIG. 6. Phase contrast imaging of tapping AFM mode distinguishes virgin $C_{32}H_{66}$ perpendicular layer (exposure time = 0 s) from parallel layer: the bright region corresponds to $C_{32}H_{66}$ perpendicular layer and the dark region corresponds to the parallel layer.

D. Enhanced stiffness of alkane thin films by bombardment

In AFM tapping mode, the phase shift can be approximately proportional to the reduced Young's modulus of the sample.⁵⁵ With the tapping condition such that the setting point is $\sim 60\%$ of the freely vibrating amplitude,⁵⁶ in the phase image of Fig. 6, we can visibly distinguish the perpendicular layer (brighter region) from the parallel layer (darker region). However, the phase shift in the tapping mode could only be qualitatively associated with mechanical property variations in the presence of viscoelasticity and/or adhesion hysteresis.⁵⁷ Tomayo and Garcia⁵⁷ theoretically and experimentally demonstrated that the phase shift is not sensitive to stiff materials of relatively large Young's modulus (approximately when the Young's modulus $E > \sim 1$ GPa) even with energy dissipation involved. At present, as shown in Fig. 6, we only can qualitatively measure the Young's modulus when the Young's modulus or the stiffness of both layers is smaller than 2 GPa before bombardment. After 700 s bombardment as shown in Fig. 7, such phase contrast can barely be differentiated. And both of these two types of layers had been stiffened with their Young's modulus $> \sim 1$ GPa.

To quantify the enhanced stiffness of bombarded layers, AFM HamoniXTM (Ref. 38) and force modulation³⁹ modes were applied to measure the Young's moduli of both perpendicular and parallel layers.^{37-39,58,59} These two modes are well complementary to each other. Although the force modulation mode can be used for measuring a large range of Young's modulus, it operates in contact mode and may damage soft samples of low stiffness. Its resolution is degraded at a high scanning speed. Recently, HamoniXTM mode, which works as torsional tapping mode using a T-shaped cantilever,

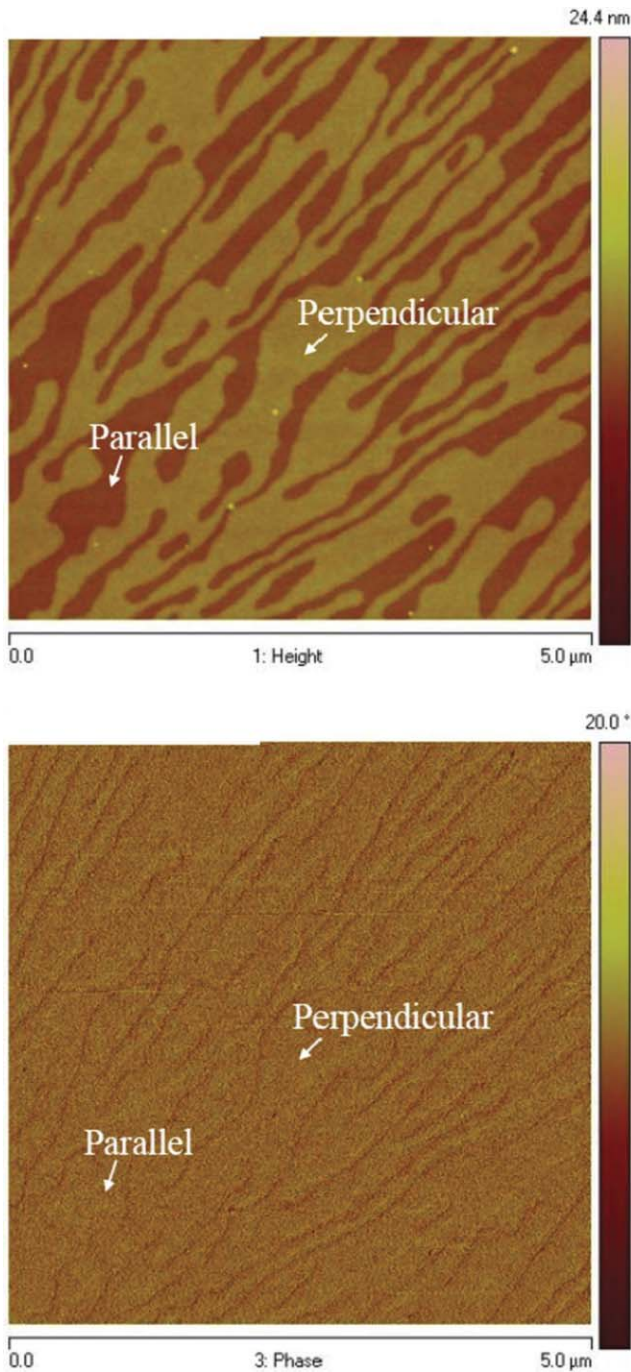


FIG. 7. Topographic (top) and phase (bottom) images of $C_{32}H_{66}$ monolayers after 700 s bombardment, where the phase image cannot effectively distinguish perpendicular layers from parallel layers because of the increased Young's moduli after hydrogen bombardment.

can measure a large dynamic range of mechanical properties from 1 MPa to 10 GPa.⁶⁰ It is a tapping mode and well suitable for measuring the parallel layers of low stiffness, much lower than the perpendicular layers. In Fig. 8, to validate HamoniXTM mode, we tested these representative materials: LDPE \sim 100 MPa, PS \sim 2 GPa, polypropylene (PP) \sim 1.2 GPa, and mica \sim 50 GPa. The measured results presented in Fig. 8 are \sim 77 MPa, \sim 1.9 GPa, \sim 1.5 GPa, and \sim 10.9 GPa, for above materials, respectively. As to the measurement of mica, HamoniXTM loses its accuracy for materials of stiffness larger

TABLE III. Young's modulus of $C_{32}H_{66}$ thin films before and after bombardment.

	Parallel layer		Perpendicular layer	
	0 s	700 s	0 s	700 s
Young's modulus by HamoniX TM (GPa)	\sim 0.2	\sim 1.0	\sim 1.2	\sim 6.5
Young's modulus by force modulation (GPa)			\sim 1.5	\sim 6.2

than 10 GPa.⁶⁰ In this work, we are applying both of force modulation and HamoniXTM to measure the Young's modulus of thin films.

HamoniXTM mode^{38,61} has been developed as an advanced tapping mode carrying the capability to quantitatively obtain stiffness contrast on heterogeneous surface with high lateral resolution. This mode resolves the tip-sample contact in time domain through analyzing the difference at higher harmonics on the broader fast Fourier transform (FFT) spectrum of tip-sample interaction, which carries rich information about the mechanical property of the surface. We applied HamoniXTM to measure the Young's moduli of virgin perpendicular layer, virgin parallel layer, and parallel layer after 700 s bombardment. As shown in Fig. 9, HamoniXTM mode can effectively distinguish these two differently oriented layers by stiffness, the parallel layer of \sim 0.2 GPa stiffness softer than the perpendicular layer of \sim 1.2 GPa stiffness. After 700 s bombardment, the parallel layer was stiffened to \sim 1.0 GPa and the perpendicular layer was stiffened to \sim 6.5 GPa (Table III).

In AFM force modulation mode, the cantilever basis is low frequency modulated while the tip is in contact with the surface. A stiffer area on the surface deforms less than a softer area and leads to a higher amplitude of cantilever deflection. According to Hertzian theory of elastic-circular-point-contact applied, the Young's modulus of the sample can be correlated with cantilever amplitudes as follows.³⁹ The compression ratio is given as

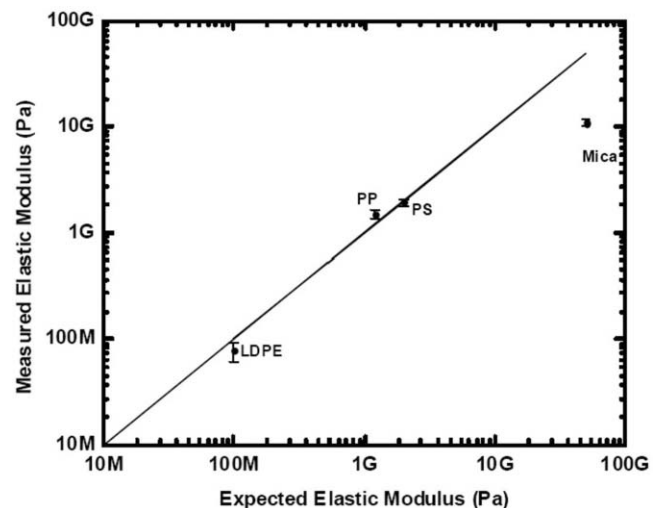


FIG. 8. Large dynamic range of nanomechanical measurements on several reference samples by the HamoniXTM mode: LDPE \sim 100 MPa, PS \sim 2 GPa, PP \sim 1.2 GPa and mica \sim 50 GPa.

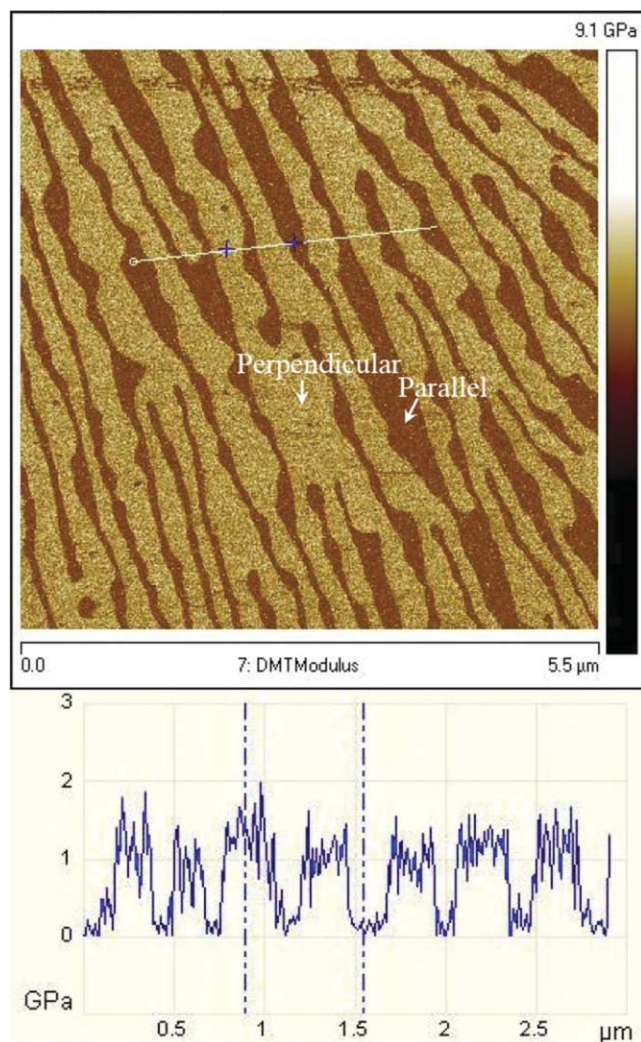


FIG. 9. Nanomechanical mapping of parallel and perpendicular layers of virgin $C_{32}H_{66}$ thin film in the HarmoniXTM mode. The upper figure shows the contrast of stiffness over the entire surface; the lower figure shows the Young's modulus profile along a section line, where the Young's modulus of perpendicular layer is ~ 1.2 GPa and that of parallel layer is ~ 0.2 GPa.

$$\varepsilon = \frac{z_c}{z_f}, \quad (2)$$

where z_c is the excitation amplitude of the cantilever and z_f is the amplitude of the cantilever exerting force on a sample with finite stiffness. Then, the Young's modulus can finally be determined by

$$E_{\text{sample}} = \frac{\varepsilon}{1 - \varepsilon} H E_{\text{tip}}, \quad (3)$$

where H is related to apparatus coefficient.³⁹ The AFM force modulation mode uses a separate piezoelectric actuator to independently activate the probe (Veeco Application; Note: force modulation imaging with atomic force microscopy). The excitation amplitude of the cantilever measured on a rigid sapphire ($E \sim 435$ GPa) is 10.51 mV, which corresponds to 2.39 nm amplitude of the cantilever with calibrated sensitivity of 227.5 ± 2.0 nm/V. The diamond tip of calibrated spring constant 0.23 N/m was modulated at the frequency of 10.86 kHz and contact deflection with sample was set at 5.23 nN. Representative amplitude curves along the scan di-

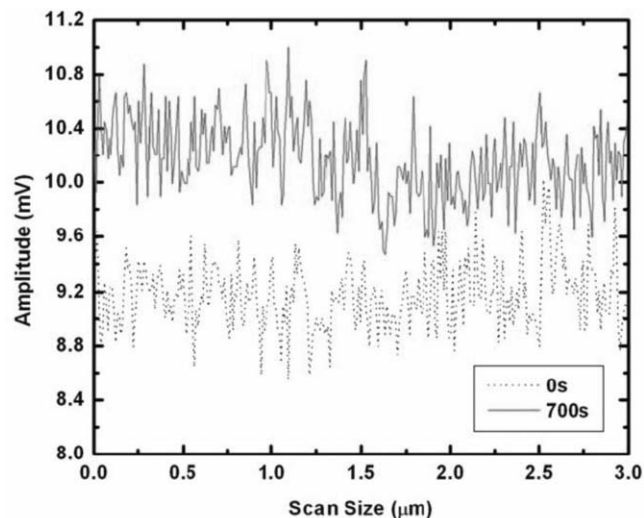


FIG. 10. Amplitudes of the AFM cantilever in force modulation on virgin $C_{32}H_{66}$ perpendicular layer (dots) and perpendicular layer bombarded for 700 s (dashes) are 9.14 and 10.17 mV, respectively.

rection with the scanning size of $3 \mu\text{m}$ are shown in Fig. 10. The averaged amplitudes are 9.17, 10.17, and 10.48 mV for perpendicular monolayer without bombardment, the perpendicular monolayer after 700 s bombardment, and SiO_2 surface, respectively. Because the Young's modulus of the SiO_2 is known as ~ 70 GPa, we can successfully obtain the constant value for $H E_{\text{tip}}$ in Eq. (3). Continuously using Eq. (3), we can easily calculate the Young's moduli for perpendicular monolayer without bombardment and the perpendicular monolayer with 700 s bombardment to be ~ 1.5 and ~ 6.2 GPa, respectively. The measured value for the virgin perpendicular monolayer (without bombardment) falls in the range as reported in literature^{58,62} and is also in a good agreement with the value measured by HarmoniXTM ~ 1.2 GPa as shown in Fig. 9. Through the proposed bombardment, stiffness of the thin film (for both perpendicular and parallel layers) can be enhanced up to five times as shown in Table III.

IV. CONCLUSIONS

A surface modification method of molecular thin films by hyperthermal hydrogen projectile bombardment technology has been implemented through selectively breaking C–H bonds of hydrocarbon chains to make carbon radicals that lead to formation of C–C bonds between hydrocarbon chains. The chemical property of the thin film was preserved in terms of the unchanged carbon concentration confirmed by XPS. Through studying morphological and mechanical properties of the thin films, the bombarded monolayers (the perpendicular layers) have been proved to possess cross-linked molecular networks and a smooth surface characterized by AFM. The mechanical strength of the thin films has been enhanced by five times. We think a carbon-rich (e.g., amorphous) layer was formed in the hydrogen bombardment process. The above-mentioned advantages of this technique are very important in improving tribological properties of modern miniaturized

systems to extend their life cycles. Wherein the enhanced stiffness has also been demonstrated on other polymeric systems such as polylactic acid films, the Young's moduli of which were prompted by ~ 8 times through 30 min bombardment (unpublished), respectively.

ACKNOWLEDGMENTS

We gratefully acknowledge the financial support from Ontario Centers of Excellence (OCE) and LANXESS Inc. J. Yang is also grateful for the support from Natural Science and Engineering Research Council of Canada (NSERC) and Canada Foundation for Innovation (CFI). And Y. Liu would appreciate the fellowship support from Ontario Graduate Scholarship (OGS).

- ¹A. Centrone, E. Penzo, M. Sharma, J. W. Myerson, A. M. Jackson, N. Marzari, and F. Stellacci, *Proc. Natl. Acad. Sci. U. S. A.* **105**, 9886 (2008).
- ²F. Caruso and H. Mohwald, *Langmuir* **15**, 8276 (1999).
- ³M. A. Reed, J. Chen, A. M. Rawlett, D. W. Price, J. M. Tour, *Appl. Phys. Lett.* **78**, 3735 (2001).
- ⁴Y. Chen, G. Y. Jung, D. A. A. Ohlberg, X. M. Li, D. R. Stewart, J. O. Jeppesen, K. A. Nielsen, J. F. Stoddart, and R. S. Williams, *Nanotechnology* **14**, 462 (2003).
- ⁵H. S. Nalwa and A. Kakuta, *Appl. Org. Chem.* **6**, 645 (1992).
- ⁶D. R. Talham, T. Yamamoto, and M. W. Meisel, *J. Phys. Condens. Matter* **20**, 184006 (2008).
- ⁷S. Yoshida, T. Ono, and M. Esashi, *Nanotechnology* **19**, 475302 (2008).
- ⁸S. Yoshida, T. Ono, S. Oi, and M. Esashi, *Nanotechnology* **16**, 2516 (2005).
- ⁹L. J. Kepley, R. M. Crooks, and A. J. Ricco, *Anal. Chem.* **64**, 3191 (1992).
- ¹⁰T. Kang, S. R. Hong, J. Moon, S. Oh, and J. Yi, *Chem. Commun. (Cambridge)* **2005**, 3721 (2005).
- ¹¹A. J. Parnell, S. J. Martin, C. C. Dang, M. Geoghegan, R. A. L. Jones, C. J. Crook, J. R. Howse, and A. J. Ryan, *Polymer* **50**, 1005 (2009).
- ¹²E. Ruckenstein and Z. F. Li, *Adv. Colloid Interface Sci.* **113**, 43 (2005).
- ¹³J. Hyun and A. Chilkoti, *Macromolecules* **34**, 5644 (2001).
- ¹⁴B. Zhao and W. J. Brittain, *J. Am. Chem. Soc.* **121**, 3557 (1999).
- ¹⁵M. Lemieux, S. Minko, D. Usov, M. Stamm, and V. V. Tsukruk, *Langmuir* **19**, 6126 (2003).
- ¹⁶W. M. Lau, *Nucl. Instrum. Methods Phys. Res. B* **131**, 341 (1997).
- ¹⁷W. M. Lau, Z. Zheng, Y. H. Wang, Y. Luo, L. Xi, K. W. Wong, and K. Y. Wong, *Can. J. Chem.* **85**, 859 (2007).
- ¹⁸Z. Zheng, X. D. Xu, X. L. Fan, W. M. Lau, and R. W. M. Kwok, *J. Am. Chem. Soc.* **126**, 12336 (2004).
- ¹⁹C. A. Andersen, H. J. Roden, and C. F. Robinson, *J. Appl. Phys.* **40**, 3419 (1969).
- ²⁰J. C. Arnold and H. H. Sawin, *J. Appl. Phys.* **70**, 5314 (1991).
- ²¹J. A. Kenney and G. S. Hwang, *J. Appl. Phys.* **101**, 044307 (2007).
- ²²J. P. Chang and J. W. Coburn, *J. Vac. Sci. Technol. A* **21**, S145 (2003).
- ²³M. K. Abatchev and S. K. Murali, *Electrochem. Solid-State Lett.* **9**, F1 (2006).
- ²⁴B. P. Linder and N. W. Cheung, *IEEE Trans. Plasma Sci.* **24**, 1383 (1996).
- ²⁵G. A. Sefler, Q. Du, P. B. Miranda, and Y. R. Shen, *Chem. Phys. Lett.* **235**, 347 (1995).
- ²⁶X. Z. Wu, E. B. Sirota, S. K. Sinha, B. M. Ocko, and M. Deutsch, *Phys. Rev. Lett.* **70**, 958 (1993).
- ²⁷H. Schollmeyer, B. Struth, and H. Riegler, *Langmuir* **19**, 5042 (2003).
- ²⁸C. Merkl, T. Pfohl, and H. Riegler, *Phys. Rev. Lett.* **79**, 4625 (1997).
- ²⁹T. Yamamoto, K. Nozaki, A. Yamaguchi, and N. Urakami, *J. Chem. Phys.* **127**, 154704 (2007).
- ³⁰K. W. Herwig, B. Matthies, and H. Taub, *Phys. Rev. Lett.* **75**, 3154 (1995).
- ³¹H. Mo, H. Taub, U. G. Volkmann, M. Pino, S. N. Ehrlich, F. Y. Hansen, E. Lu, and P. Miceli, *Chem. Phys. Lett.* **377**, 6 (2003).
- ³²F. W. DelRio, K. L. Steffens, C. Jaye, D. A. Fischer, and R. F. Cook, *Langmuir* **26**, 1688 (2010).
- ³³O. Marti, H. O. Ribi, B. Drake, T. R. Albrecht, C. F. Quate, and P. K. Hansma, *Science* **239**, 50 (1988).
- ³⁴K. Morigaki, H. Schonherr, C. W. Frank, and W. Knoll, *Langmuir* **19**, 6994 (2003).
- ³⁵G. Oncins, C. Vericat, and F. Sanz, *J. Chem. Phys.* **128**, 044701 (2008).
- ³⁶Q. Zhong, D. Inniss, K. Kjoller, and V. B. Elings, *Surf. Sci.* **290**, L688 (1993).
- ³⁷M. D. Dong, S. Husale, and O. Sahin, *Nat. Nanotechnol.* **4**, 514 (2009).
- ³⁸O. Sahin, S. Magonov, C. Su, C. F. Quate, and O. Solgaard, *Nat. Nanotechnol.* **2**, 507 (2007).
- ³⁹M. Radmacher, R. W. Tilmann, and H. E. Gaub, *Biophys. J.* **64**, 735 (1993).
- ⁴⁰W. M. Lau and R. W. M. Kwok, *Int. J. Mass. Spectrom.* **174**, 245 (1998).
- ⁴¹L. Xi, Z. Zheng, N. S. Lam, O. Grizzi, and W. M. Lau, *Appl. Surf. Sci.* **254**, 113 (2007).
- ⁴²S. Alexander, L. Hellemans, O. Marti, J. Schneir, V. Elings, P. K. Hansma, M. Longmire, and J. Gurley, *J. Appl. Phys.* **65**, 164 (1989).
- ⁴³G. Meyer and N. M. Amer, *Appl. Phys. Lett.* **53**, 1045 (1988).
- ⁴⁴J. L. Hutter and J. Bechhoefer, *Rev. Sci. Instrum.* **64**, 3342 (1993).
- ⁴⁵U. G. Volkmann, M. Pino, L. A. Altamirano, H. Taub, and F. Y. Hansen, *J. Chem. Phys.* **116**, 2107 (2002).
- ⁴⁶A. Holzwarth, S. Leporatti, and H. Riegler, *Europhys. Lett.* **52**, 653 (2000).
- ⁴⁷H. Mo, S. Trogisch, H. Taub, S. N. Ehrlich, U. G. Volkmann, F. Y. Hansen, and M. Pino, *Phys. Status Solidi A* **201**, 2375 (2004).
- ⁴⁸M. Bai, S. Trogisch, S. Magonov, and H. Taub, *Ultramicroscopy* **108**, 946 (2008).
- ⁴⁹H. Siringhaus, N. Tessler, and R. H. Friend, *Synth. Met.* **102**, 857 (1999).
- ⁵⁰S. Trogisch, M. J. Simpson, H. Taub, U. G. Volkmann, M. Pino, and F. Y. Hansen, *J. Chem. Phys.* **123**, 154703 (2005).
- ⁵¹B. Bhushan, *Handbook of Micro/Nano Tribology*, 2nd ed. (CRC Press, Boca Raton, 1999).
- ⁵²M. Hartig, L. F. Chi, X. D. Liu, and H. Fuchs, *Thin Solid Films* **329**, 262 (1998).
- ⁵³G. J. Simpson, D. L. Sedin, and K. L. Rowlen, *Langmuir* **15**, 1429 (1999).
- ⁵⁴V. V. Tsukruk, I. Luzinov, and D. Julthongpipit, *Langmuir* **15**, 3029 (1999).
- ⁵⁵S. N. Magonov, V. Elings, and M. H. Whangbo, *Surf. Sci.* **375**, L385 (1997).
- ⁵⁶S. N. Magonov and D. H. Reneker, *Annu. Rev. Mater. Sci.* **27**, 175 (1997).
- ⁵⁷J. Tamayo and R. Garcia, *Appl. Phys. Lett.* **71**, 2394 (1997).
- ⁵⁸W. J. Price, S. A. Leigh, S. M. Hsu, T. E. Patten, and G. Y. Liu, *J. Phys. Chem. A* **110**, 1382 (2006).
- ⁵⁹R. M. Overney, E. Meyer, J. Frommer, H. J. Guntherodt, M. Fujihira, H. Takano, and Y. Gotoh, *Langmuir* **10**, 1281 (1994).
- ⁶⁰O. Sahin and N. Erina, *Nanotechnology* **19**, 445717 (2008).
- ⁶¹S. D. Solares and H. Hölscher, *Nanotechnology* **21**, 075702 (2010).
- ⁶²F. W. DelRio, C. Jaye, D. A. Fischer, and R. F. Cook, *Appl. Phys. Lett.* **94**, 131909 (2009).